Article:
Shaw, R.A. and Hill, J.G. (2017) Prescreening and efficiency in the evaluation of integrals over ab initio effective core potentials. Journal of Chemical Physics, 147 (7). 074108 .
ISSN: 0021-9606

https://doi.org/10.1063/1.4986887

Prescreening and efficiency in the evaluation of integrals over ab initio effective core potentials

Robert A. Shaw[1] and J. Grant Hill[1, a)]

Department of Chemistry, University of Sheffield, Sheffield S3 7HF, U.K.

(Dated: 31 July 2017)

New, efficient schemes for the prescreening and evaluation of integrals over effective core potentials (ECPs) are presented. The screening is shown to give a rigorous, and close bound, to within on average 10% of the true value. A systematic rescaling procedure is given to reduce this error to approximately 0.1%. This is then used to devise a numerically stable recursive integration routine that avoids expensive quadratures. Tests with CCSD(T) calculations on small silver clusters demonstrate that the new schemes show no loss in accuracy, while reducing both the power and prefactor of the scaling with system size. In particular, speedups of roughly 40 times can be achieved compared to quadrature-based methods.

[a)]Electronic mail: grant.hill@sheffield.ac.uk

I. INTRODUCTION

Ab initio quantum chemistry methods are nowadays widely used for the accurate study of the properties and dynamics of molecular systems.[1,2] They offer insight into difficult problems with a level of detail that would often be impossible to obtain experimentally. However, for the most accurate methods the unfavourable scaling of computational cost with system size - specifically, the number of electrons and basis functions - prohibits their use for many interesting cases. Several techniques and approximations[3–5] have been introduced to counteract this, one of the earliest being the observation that only the valence electrons are of significance in many chemical applications.[6–9] In heavy atoms in particular[10], the innermost electrons are largely unperturbed by the surrounding environment. This suggests that a prudent way to reduce the complexity of the problem is to freeze these electrons, treating them only in an averaged way. This led to the idea of a pseudopotential[11], or specifically in the case of *ab initio* methods, an effective core potential (ECP).[12] This treats the potential associated with the core electrons as being fixed, significantly improving the efficiency of the calculation, and only requiring the additional calculation of integrals over a one-electron, three-center operator.

In addition to the computational savings, using an ECP allows for a simple way of including scalar relativistic effects into what would otherwise be a non-relativistic Schrödinger equation.[13] For heavier atoms, the electrons closest to the nucleus (i.e. the core electrons) have substantial relativistic character, meaning that neglecting these effects can lead to significant errors.[14–17] While methods do exist to include such terms in a calculation, it is much more efficient to include them in the fitting process of the ECP. In this way, the accuracy of results may even be improved[18,19], despite a substantial number of electrons being frozen.

As first proposed by Goddard[20] and then improved by Kahn and coworkers[21,22], the ECP is generally fitted to the following form:

$$U(\mathbf{r}) = U_L(r) + \sum_{\lambda=0}^{L-1} \sum_{\mu=-\lambda}^{\lambda} |S_{\lambda\mu}\rangle \, U_\lambda(r) \, \langle S_{\lambda\mu}| \tag{1}$$

where the angular momentum, λ, of the radial shells U_λ ranges from zero to L, and $S_{\lambda\mu}$ is a real spherical harmonic. The $U_l(r)$ are normally expanded in terms of Gaussian functions:

$$U_l(r) = \sum_k d_{kl} r^{n_{kl}} \exp\left(-\zeta_{kl} r^2\right) \tag{2}$$

The coefficients d_{kl}, powers n_{kl}, and exponents ζ_{kl} in general depend on the angular momentum of the shell being fitted. This potential is then added as a modification to the usual core Hamiltonian, which becomes (in atomic units)

$$H_0 = -\frac{1}{2}\nabla^2 - \sum_{iA}\left[\frac{Z_A^{\text{eff}}}{R_{iA}} - U^A(\mathbf{r})\right] \tag{3}$$

where i, A denote an electron and nucleus, respectively, Z_A^{eff} is the effective nuclear charge, which is the usual nuclear charge minus the number of core electrons, and the potential U^A is the ECP on center A, taken to be zero if there is no such ECP. The resulting new integrals are thus of two different varieties: those involving projections with real spherical harmonics, termed Type II, and those that do not, termed Type I. Due to the summation in equation 1, there are far more of the former than there are of the latter, and as such it is these that take up the bulk of the computational effort.

Several different schemes have been devised for the evaluation of these integrals. Of particular early significance were the methods due to Kahn[22] and McMurchie[23]. The exposition of the latter will be summarised in the next section. This scheme was improved first by Skylaris *et al.*[24], then Flores-Moreno and coworkers[25], who introduced a half-numerical approach involving adaptive quadrature over the radial integrals. More recently, Song *et al.* have suggested a way to prescreen these integrals while developing their rapid computation on graphical processing units.[26,27] A few attempts have been made to avoid the need for quadrature, most notably by McMurchie[23], Kolar[28], and Bode[29]. These made use of recurrence relations, but have largely been neglected for a number of reasons. The earliest such approaches suffered from severe numerical problems[25], due to both the limitations of the machines available at the time, and the particular choices of relations. The most recent was more successful[29], but was superseded by the half-numerical scheme as the latter ran the quadrature over contracted basis functions, as opposed to over all combinations of primitives.

In the current work, we present both an improved method for prescreening the radial integrals and a new recursive method for their evaluation. The scheme does not suffer from numerical issues on modern architectures, and a code generation procedure is presented that unrolls the recursions, allowing for their extremely efficient evaluation. As such, this approach is found to be significantly quicker than the half-numerical one, despite being over primitive functions. In addition, the prescreening scheme is found to lead to speedups when

applied to either method, and the scaling of both approaches with system size can be seen to become less steep. These therefore represent an improvement to existing integration routines that will allow for faster calculations on large systems.

II. ECP INTEGRALS

Here we briefly summarise the expansion of the ECP matrix elements in terms of angular and radial integrals, as described in more detail in other sources[23,25]. As noted above, taking the matrix element over equation 1 results in two types of integral. The first of these (Type I), not involving projections, requires minimal effort and thus will not be considered here. We consider matrix elements of the Type II integrals over Gaussian-type basis functions. The function ϕ_a, with angular momentum a and located at $\mathbf{A}$, is defined in the usual way as

$$\phi_a(\mathbf{r}) = x_A^{a_x} y_A^{a_y} z_A^{a_z} \sum_i d_{ia} e^{-\zeta_{ia} r_A^2} \tag{4}$$

where $\alpha_A = r\alpha - A_\alpha$ for $\alpha = x, y, z$, $r_A = |\mathbf{r} - \mathbf{A}|$, and d_{ia}, ζ_{ia} are the primitive coefficients and exponents, respectively. The matrix element, $\chi_{ab}^{\lambda\mu}$, is given by

$$\begin{aligned} \chi_{ab}^{\lambda\mu} &= \langle\phi_a| \left(|S_{\lambda\mu}\rangle\, U_\lambda(r)\, \langle S_{\lambda\mu}|\right) |\phi_b\rangle \\ &= \int_0^\infty dr\ r^2 U_\lambda(r) \int_\Omega d\Omega\ \phi_a(\mathbf{r}) S_{\lambda\mu} \int_{\Omega'} d\Omega'\ \phi_b(\mathbf{r}') S_{\lambda\mu} \end{aligned} \tag{5}$$

This involves two integrals over solid angles, Ω and Ω', of the same form:

$$T_a^{\lambda\mu} = \int_\Omega d\Omega\ \phi_a(\mathbf{r}) S_{\lambda\mu} \tag{6}$$

We introduce equation 4 into this and use the binomial expansion for the powers of α_A. Remembering $a = a_x + a_y + a_z$, and defining $a_{klm} = k + l + m$, this therefore becomes

$$\begin{aligned} T_a^{\lambda\mu} = \sum_i d_{ia} \sum_{k=0}^{a_x} \sum_{l=0}^{a_y} \sum_{m=0}^{a_z} (-1)^a C_k^{x,A} C_l^{y,A} C_m^{z,A} e^{-\zeta_{ia} A^2} \\ \times r^{a_{klm}} e^{-\zeta_{ia} r^2} \int_\Omega d\Omega\ x^k y^l z^m e^{2\zeta_{ia} \mathbf{A}\cdot\mathbf{r}} S_{\lambda\mu} \end{aligned} \tag{7}$$

where the coefficients $C_i^{\alpha,A}$ are defined as

$$C_i^{\alpha,A} = (-1)^i \binom{a_\alpha}{i} A_\alpha^{a_\alpha - i} \tag{8}$$

The exponential of the dot product in the remaining integral in equation 7 can be expanded in terms of real spherical harmonics and modified spherical Bessel functions of the first kind[30], M_λ, to give

$$\begin{aligned}\int_\Omega d\Omega\ x^k y^l z^m e^{2\zeta_{ia}\mathbf{A}\cdot\mathbf{r}} S_{\lambda\mu} \\ = 4\pi \sum_{\rho=0}^{\infty} M_\rho(2\zeta_{ia}Ar) \sum_{\sigma=-\rho}^{\rho} S^A_{\rho\sigma}\Omega^{klm}_{\rho\sigma,\lambda\mu}\end{aligned} \tag{9}$$

Here, we have used the notation $S^A_{\rho\sigma} = S_{\rho\sigma}(\theta_A, \phi_A)$, and defined the angular integral

$$\Omega^{klm}_{\rho\sigma,\lambda\mu} = \int_\Omega d\Omega\ x^k y^l z^m S_{\rho\sigma} S_{\lambda\mu} \tag{10}$$

which can easily be evaluated analytically. In particular, it is necessarily only non-zero for $|\rho{-}k{-}l{-}m| \leq \lambda \leq \rho{+}k{+}l{+}m$, and $k{+}l{+}m{+}\rho{-}\lambda$ even. The former restricts the otherwise infinite summation in equation 9, while the latter allows for the more efficient generation of the total integrals, as many radial integrals can be neglected. Note also that this angular integral does not depend at all on the particular exponents or contraction coefficients of the basis functions, and thus can be tabulated in advance.

Using the shorthand $D^A_{klm} = C^{x,A}_k C^{y,A}_l C^{z,A}_m$, the Type II integral, equation 5, can therefore be written as

$$\begin{aligned}\chi^{\lambda\mu}_{ab} =& 16\pi^2 \sum_{klm} D^A_{klm} \sum_{pqr} D^B_{pqr} \\ &\times \sum_{\rho\sigma\kappa\tau} S^A_{\rho\sigma} S^B_{\kappa\tau} \Omega^{klm}_{\rho\sigma,\lambda\mu} \Omega^{pqr}_{\kappa\tau,\lambda\mu} \mathcal{T}^{2+a_{klm}+b_{pqr}+n_{k\lambda}}_{\rho\kappa\lambda}\end{aligned} \tag{11}$$

We have defined the contracted radial integral as

$$\mathcal{T}^N_{\rho\kappa\lambda} = \sum_{ijk} d_{ia} d_{jb} d_{k\lambda} \exp(-\zeta_{ia}A^2 - \zeta_{jb}B^2) \mathcal{Q}^N_{\rho\kappa\lambda} \tag{12}$$

which in turn is in terms of the primitive radial integral

$$\mathcal{Q}^N_{\rho\kappa\lambda} = \int_0^\infty dr\ r^N e^{-p_{ijk}r^2} M_\rho(2\zeta_{ia}Ar) M_\kappa(2\zeta_{jb}Br) \tag{13}$$

where $p_{ijk} = \zeta_{ia} + \zeta_{jb} + \zeta_{k\lambda}$.

Equation 13 has been found not to be very stable with respect to quadrature schemes[25], so usually an enveloped Bessel function is defined as $K_n(z) = e^{-z} M_n(z)$, and the exponential

in equation 12 is absorbed into the integrand. This then gives

$$\begin{aligned}\mathcal{R}^N_{\rho\kappa\lambda} = \int_0^\infty dr\ r^N e^{-\zeta_{k\lambda}r^2} K_\rho(2\zeta_{ia}Ar) K_\kappa(2\zeta_{jb}Br) \\ \times \exp\left(-\zeta_{ia}(r-A)^2 - \zeta_{jb}(r-B)^2\right)\end{aligned} \tag{14}$$

Flores-Moreno *et al.*[25] went further and noted that one could directly evaluate the contracted integral by quadrature by defining

$$\mathcal{K}^a_\rho(r) = \sum_i d_{ia} K_\rho(2\zeta_{ia}Ar) \tag{15}$$

and not expanding the ECP, such that equation 12 becomes

$$\begin{aligned}\mathcal{T}^N_{\rho\kappa\lambda} = \int_0^\infty dr\ r^N U_\lambda(r) \mathcal{K}^a_\rho(r) \mathcal{K}^b_\kappa(r) \\ \times \exp\left(-\zeta_{ia}(r-A)^2 - \zeta_{jb}(r-B)^2\right)\end{aligned} \tag{16}$$

Clearly, this reduces the number of individual quadratures that need to be carried out. It does not, however, reduce the number of expensive evaluations of the Bessel functions, and it also suffers significant numerical instabilities for certain arguments of the Bessel functions, as will be discussed later. In these cases where equation 16 does not converge sufficiently well, the procedure must default back to the evaluation over primitives, generally using a much tighter integration grid. Thus, even within this scheme, it is desirable to be able to efficiently screen these integrals, so that lengthy quadratures can be avoided, and to have a more efficient method for the integration over primitives.

III. PRESCREENING THE RADIAL INTEGRALS

Song *et al.* have recently suggested a method for screening the total Type II integral in equation 11.[26] They demonstrated that a substantial number of integrals can be neglected in this way. By consideration of the radial integral specifically, however, we can achieve a much closer bound. Clearly, screening the entire integral should be somewhat more efficient, but the radial integration is by far the most expensive part of the calculation, such that there is no real difference in efficiency. Moreover, achieving a tighter bound not only compensates for this, but is also crucial in the integration scheme that follows, as will be discussed later.

We begin by considering the integrand, $f(r; a, b, N)$, of equation 14 in the following,

notationally simplified form:

$$\begin{aligned} f(r;\rho,\kappa,N) &= r^N K_\rho(k_A r) K_\kappa(k_B r) \\ &\quad \times \exp\left[-\eta r^2 - \alpha(r-A)^2 - \beta(r-B)^2\right] \end{aligned} \tag{17}$$

where $k_A = 2\alpha A$, $k_B = 2\beta B$, with α, β, and η replacing ζ_{ia}, ζ_{jb}, and $\zeta_{k\lambda}$ respectively. It is shown rigorously in the supplementary material that this distribution is unimodal, and that, using the following recurrence relations[30]:

$$M_{n-1}(z) - M_{n+1}(z) = \frac{2n+1}{z} M_n(z) \tag{18}$$

$$nM_{n-1}(z) + (n+1)M_{n+1}(z) = (2n+1)M_n'(z) \tag{19}$$

it is possible to determine this mode using the transcendental equation given in equation 20.

$$\begin{aligned} 2pr_0^2 =& N - \rho - \kappa - 2 \\ &+ \left[k_A + k_B + \frac{M_{\rho-1}(k_A r_0)}{M_\rho(k_A r_0)} + \frac{M_{\kappa-1}(k_B r_0)}{M_\kappa(k_B r_0)}\right] r_0 \end{aligned} \tag{20}$$

We denote this mode as P.

At this point, it simplifies matters to rescale the distribution by this maximum and consider $g(r) = f(r)/f(P)$. This is given by

$$\begin{aligned} g(r) &= \left(\frac{r}{P}\right)^N \frac{K_\rho(k_A r)}{K_\rho(k_A P)} \frac{K_\kappa(k_B r)}{K_\kappa(k_B P)} \\ &\quad \times \exp\left[-p(r-P)^2 - (2pP + k_A + k_B)r + (k_A + k_B)P\right] \end{aligned} \tag{21}$$

If we consider a point r in the neighbourhood of the maximum, P, such that $x = r/P \approx 1$, the Bessel function ratios above are less than or equal to unity, giving the inequality

$$g(r) \leq u(x) \exp\left[-p(r-P)^2\right] \tag{22}$$

where

$$\begin{aligned} u(x) &= x^N \exp\left\{P\left[-(2pP + k_A + k_B)x + k_A + k_B\right]\right\} \\ &\approx \exp\left[-2pP^2\right] \end{aligned} \tag{23}$$

That is, in the vicinity of the maximum we have $u(x) < 1$ (as $P \neq 0$), such that $g(r) < \exp[-p(r-P)^2]$. By the analysis earlier, g is asymptotically dominated by the same Gaussian, and the monotonicity of each thus entails that $g(r) \leq \exp[-p(r-P)^2]$ on the whole

domain (note that equality occurs at the maximum, hence the weak inequality). That is, we can write that $f(r) \leq f(P)\exp[-p(r-P)^2]$, such that the primitive radial integral is bounded by

$$\begin{aligned}\mathcal{R}^N_{\rho\kappa\lambda} &\leq f(P;\rho,\kappa,N)\int_0^\infty dr\ \exp[-p(r-P)^2] \\ &= \frac{1}{2}f(P;\rho,\kappa,N)\sqrt{\frac{\pi}{p}}\left\{1+\mathrm{erf}(\sqrt{p}P)\right\}\end{aligned} \tag{24}$$

Assuming that the position of the maximum is known, this can be rapidly evaluated, either using one of the many efficient implementations of the error function, or simply using the fact that the error function is strictly increasing, such that an adequate bound can be achieved through a pretabulated point close to, but greater than, $\sqrt{p}P$. The evaluation of $f(P)$ requires two Bessel function values, as compared with the 512 needed on a typical small quadrature grid (or typically 2048 in the case where the smaller quadrature fails). Unfortunately, the transcendental nature of equation 20 means that the maximum cannot be found in closed form. However, that equation as written is a stable iterative fixed point equation, and given a close guess to P will typically converge to a sufficiently accurate value within two to three iterations, as will be demonstrated later. As each iteration requires only four additional evaluations of Bessel functions, this is still an insubstantial cost compared to the full quadrature.

Example integrands and their approximants are shown in Figure 1, where it can be seen how closely they match. In fact, from the figure it appears that simply decreasing the width of the Gaussian could result in even better agreement with the true integral. If we consider the kernel of the right hand side of equation 24 to be a function, $\tilde{R}$, of some width-controlling exponent γ, we can investigate how the error behaves as a function of this width. For simplicity we rescale the system without loss of generality, such that $P = 1$ and $f(P) = 1$. Therefore, the approximate integral as a function of γ is:

$$\tilde{R}(\gamma) = \frac{1}{2}\sqrt{\frac{\pi}{\gamma}}\left\{1+\mathrm{erf}(\sqrt{\gamma})\right\} \tag{25}$$

The monotonicity of $\mathcal{R}$ and $\tilde{R}$ then implies there is precisely one value of γ such that $\tilde{R} = \mathcal{R}$. This suggests that an ad hoc scaling of the width, or of the integral itself, could yield very good approximations to the integrals with essentially no additional effort.

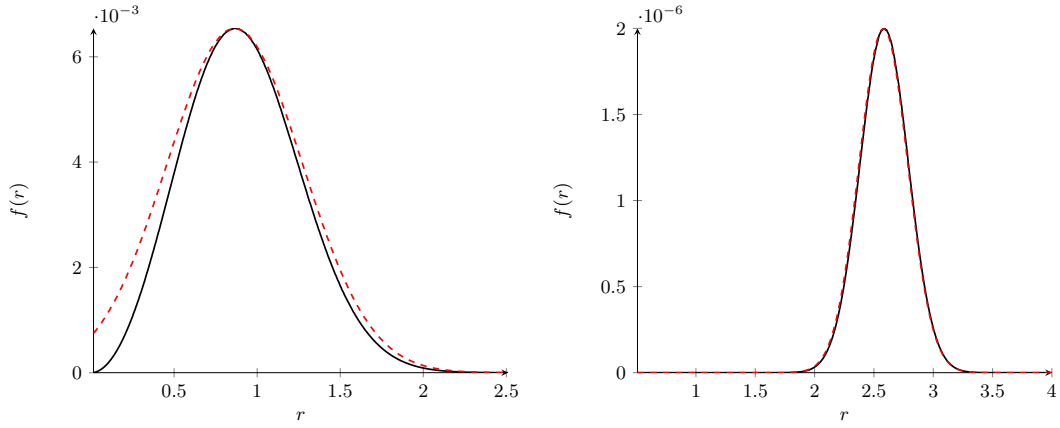

FIG. 1. Example integrands, $f(r)$ (solid black lines), and their Gaussian approximants (dashed red lines). The randomly selected parameters $(N, \rho, \kappa, p, A, B)$ are $(2, 0, 0, 3, 0.2, 2.9)$ on the left, and $(4, 0, 2, 11.8, 1.3, 3.7)$ on the right. The matching of the maxima results in a close fit, and the right hand case demonstrates the general trend towards exact agreement as the parameters k_A and k_B become larger.

IV. INTEGRATION SCHEME

As has been noted previously[23,28,29], there are a number of possible recurrences on the Bessel functions that can be used to try and evaluate the primitive radial integrals. However, for this approach to be feasible, care has to be taken in choosing not only which relations to use, but also the order to use them in, as this will have a significant impact on the numerical stability of the algorithm. In addition, precise consideration must be given to the cancellation of terms, both to avoid increasingly large alternating series and to ensure that evaluation is as efficient as possible.

Firstly, we revert to equation 13, but written in the following simplified notation, for reasons of clarity:

$$Q_{ijk} = \int_0^\infty dr\ r^k e^{-pr^2} M_i(2\alpha A r) M_j(2\beta B r) \tag{26}$$

where as always $p = \eta + \alpha + \beta$ is the sum of exponents. The symmetry of the integral with respect to interchange of a and b (and therefore i and j) means that we can, without loss of generality, assume that $j \geq i$. In addition, we note that $k \geq 2$ must always be true. Then, we reduce the first index, i, to zero by combining equations 18 and 19, this time so as to eliminate M_{n-1}:

$$M_{n+1}(z) = M_n'(z) - \frac{n}{z} M_n(z) \tag{27}$$

Note that division (multiplication) by r corresponds to decreasing (increasing) the index k by one. Using this, the fact that the integrand necessarily goes to zero at the integration limits, and the result earlier for the derivative of the j-indexed Bessel function, integration by parts then gives the following relation for Q_{ijk}:

$$Q_{ijk} = \mu_{ijk} Q_{i-1,j,k-1} + \nu Q_{i-1,j-1,k} + \xi Q_{i-1,j,k+1} \tag{28}$$

where $\mu_{ijk} = (2+j-i-k)/(2\alpha A)$, $\nu = -\beta B/(\alpha A)$, and $\xi = p/(\alpha A)$. Applying this i times will reduce the first index to zero, leaving the second and third indices in the ranges $[j-i, j]$ and $[k-i, k+i]$, respectively. In this way, we avoid either increasing the second index, or reducing it below zero, as we have assumed $j \geq i$.

At this point, we can apply equation 18 directly on j to get the following:

$$Q_{0jk} = \sigma Q_{0,j-2,k} + \rho_j Q_{0,j-1,k-1} \tag{29}$$

where $\rho_j = -(2j-1)/(2\beta B)$, and $\sigma = 1$. This is included here only to simplify the process of expanding the recurrences later. This recurrence on its own is known to be quite numerically unstable when used repeatedly[25], due to the formation of an alternating series of differences, while equation 28 is more robust. Therefore, while it may seem attractive to use the former for both the i and j indices, as it will reduce said indices independently, putting the majority of the effort into the latter alleviates some potential problems. The above can be used to reduce j to either zero or unity, depending on its parity, yielding values of k from $k-j$ to k. When coupled with the earlier ranges, this implies we have integrals of the form Q_{00N} and Q_{01N} with N taking integer values in the range $[k-i-j, k+i]$. Integrals of these form are simple to evaluate analytically, using the fact that the functional forms of the first two modified spherical Bessel functions of the first kind are given by $M_0(z) = \sinh(z)/z$ and $M_1(z) = [z\cosh(z) - \sinh(z)]/z^2$.[31]

We define the following base integrals:

$$F_N = \int_0^\infty dr\ r^{N-2} e^{-pr^2} \sinh(k_A r) \sinh(k_B r) \tag{30}$$

$$G_N^B = \int_0^\infty dr\ r^{N-2} e^{-pr^2} \sinh(k_A r) \cosh(k_B r) \tag{31}$$

$$H_N = \int_0^\infty dr\ r^{N-2} e^{-pr^2} \cosh(k_A r) \cosh(k_B r) \tag{32}$$

where G_N^A is equivalently defined to G_N^B, but with the $k_A r = 2\alpha A r$ and $k_B r = 2\beta B r$ arguments exchanged. From this and the definitions of the Bessel functions, we clearly have

that $Q_{00N} \equiv F_N/(k_A k_B)$, and

$$Q_{01N} = \frac{1}{k_A k_B}\left[\upsilon G_N^B + \omega F_{N-1}\right] \tag{33}$$

where $\omega = -1/k_B$ and $\upsilon = 1$. Thus all integrals can be written in terms of the above base integrals. The lowest N, $k-i-j$, will always be of F-type, and the required integrals will alternate between F and G, up to $N = k+i$.

The solutions to these integrals are as follows, where we assume that N is even for F_N and H_N, and odd for G_N:

$$I_{2n}^{\pm} = \frac{1}{4}\sum_{m=0}^{n-1}\binom{2n-2}{2m} p^{-n_m}\Gamma(n_m) X_{2m}^{\pm} \tag{34}$$

$$G_{2n+1}^{B} = \frac{1}{4}\sum_{m=0}^{n-1}\binom{2n-1}{2m+1} p^{-n_m}\Gamma(n_m) X_{2m+1}^{-} \tag{35}$$

$$X_N^{\pm} = P_+^N e^{pP_+^2} \pm P_-^N e^{pP_-^2} \tag{36}$$

where we have defined $P_\pm = (\beta B \pm \alpha A)/p$, $F_N = I_N^-$, $H_N = I_N^+$, $n_m = n - m - 1/2$, and Γ is the gamma function.We note that these are all very similar in form, and the terms in the sums can be computed incrementally. Moreover, the gamma function values are all integer multiples of a half, and thus high-accuracy values can be hardcoded. This means that all of the necessary base integrals can be very rapidly computed in batches. The derivations for these are given in the supplementary material, along with the solutions for the other parity. The latter are more complicated, yielding incomplete gamma functions that, while not particularly difficult to compute, would not be able to be pretabulated. However, as was noted earlier, the angular parts of the integral in equation 11 are only nonzero for (using the current notation) $k+n+i+j-2\lambda$ even, where n is the power of r associated with the ECP. This is of course equivalent to requiring that $k+n-i-j$ be even, which so long as n is even, will result in only even N for the F-type integrals, and odd N for the G-type. It happens to be the case that for the vast majority of ECPs, n is even; in fact, it is usually zero. Note that the factor of two from the spherical volume element is often included in the power, so that the basis may appear to have a power of two - we are explicitly including it here.

However, the above formulas only apply for $N \geq 2$, as the binomial expansion used is in general not valid over the whole domain of the integral for negative powers. A number

of integrals do involve $k-i-j<0$, and so we must find further recurrences to determine these. This can easily be done using integration by parts on the power of r, yielding:

$$F_N = \frac{2p}{N-1}F_{N+2} - \frac{k_A}{N-1}G^A_{N+1} - \frac{k_B}{N-1}G^B_{N+1} \tag{37}$$

$$G^{A/B}_N = \frac{2p}{N-1}G^{A/B}_{N+2} - \frac{k_{B/A}}{N-1}H_{N+1} - \frac{k_{A/B}}{N-1}F_{N+1} \tag{38}$$

$$H_N = \frac{2p}{N-1}H_{N+2} - \frac{k_B}{N-1}G^A_{N+1} - \frac{k_A}{N-1}G^B_{N+1} \tag{39}$$

The only remaining problem is the case where $N=1$, when the above clearly cannot work. Under the assumption that odd N only occurs for the G-type integrals, we only need explicitly derive G_1, which is as follows:

$$G^B_1 = \frac{1}{2}\sqrt{\pi}\left\{e^{pP_+^2}D(\sqrt{p}P_+) - e^{pP_-^2}D(\sqrt{p}P_-)\right\} \tag{40}$$

where $D(z)$ is the Dawson function[30], closely related to the error function. This adds a small amount of complication, but highly accurate and efficient implementations of the Dawson function are readily available, and only up to four such evaluations are needed (G^A_1 and G^B_1). The derivation of the above is given in the supplementary material, along with both F_1 and H_1 for completeness. It should be pointed out that, in the case where one of the positions is zero (i.e. k_A or k_B are zero), the above scheme needs to be modified slightly; the details of these special cases are also given in the supplementary material.

A. Unrolling the recurrence relations

The ability to write integrals involving arbitrary angular momenta in terms of simple functions is useful, but not in itself a guarantee of efficiency. From a programmatic standpoint, recursion is in general much slower than iteration; on top of this, repeatedly taking differences of similarly sized quantities can easily cause problems unless extremely high-precision arithmetic is employed. The solution to both of these issues is to explicitly expand the terms in the recursions such that any given integral can be written as

$$Q_{ijk} = \sum_{m=k-i-j}^{k+i}\left\{c_{m,F}F_m + c_{m,G}G_m + c_{m,H}H_m\right\} \tag{41}$$

where the coefficients, $c_{m,X}$ are to be determined. This then requires a minimum of evaluations, allowing for extensive optimisation, and if the form of the coefficients can be simplified, the number of arithemetic operations can be minimised.

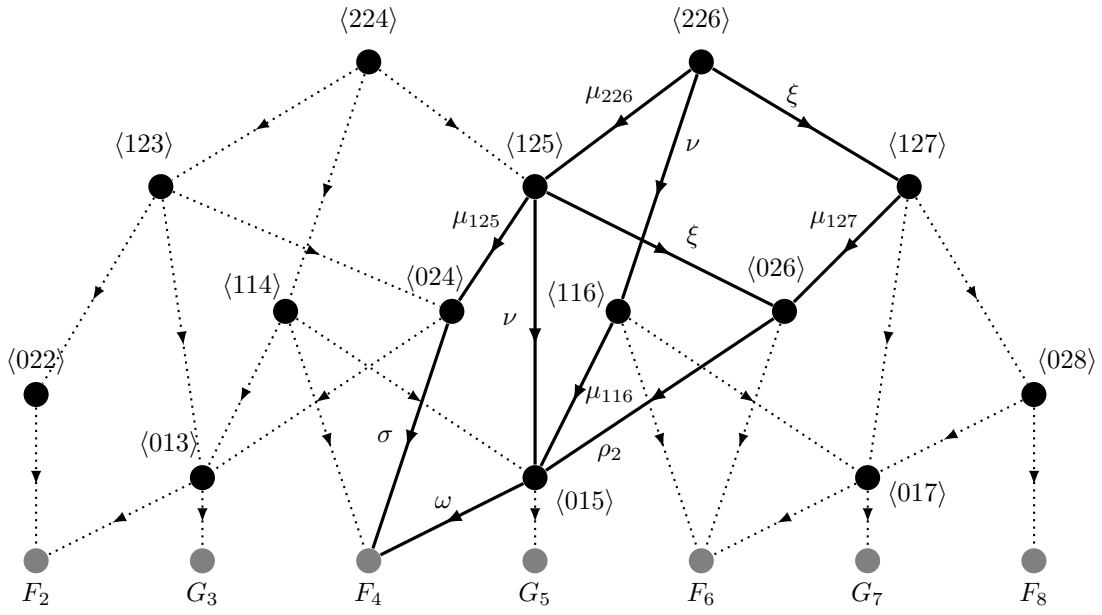

FIG. 2. A subgraph of the infinite three-dimensional network defined by the recursion relations, as described in the text. The directed edges are indicated with arrowed, dotted lines, with the vertices (integrals) shown by solid black circles labelled with their indices, $\langle ijk \rangle$. Base integrals are shown by the grey vertices. The solid edges demonstrate the five distinct paths from $\langle 226 \rangle$ to F_4; for clarity, only these edges are labelled with their weights (coefficients).

In order to generate the correct coefficients, it is necessary to enumerate all possible routes from the starting indices, ijk, to the base integral, X_m. This is a combinatorial problem equivalent to finding all distinct connecting paths on a digraph with edges defined by the recursive 'rules' set out above. That is, the index i is reduced first using relation 28, followed by j using equation 29, before finally utilising equation 33. One could include then expanding the negative-indexed base integrals at this point, or could treat those separately and assume that all indices of base integral are available. It is somewhat simpler to take the latter approach, and this is shown for a subgraph in Figure 2.

The class of edge can be denoted by the constant - μ, ν, or ξ (for the first index), and ρ, σ, υ, or ω (for the second index) - associated with a given term, weighted by its index changes, $(\Delta i, \Delta j, \Delta k)$. These changes are $(-1, 0, -1)$, $(-1, -1, 0)$, $(-1, 0, +1)$, $(0, -1, -1)$, $(0, -2, 0)$, $(0, -1, 0)$, and $(0, -1, -1)$, respectively, as can be seen by inspection of either the recurrence relations or the network in Figure 2. The path through the graph can thus be written as a list of edges traversed; for example, $[\mu\mu\nu\rho\omega]$. Given the starting vertex, $\langle ijk \rangle$,

TABLE I. Enumeration of all paths, and the resulting coefficients for the base integrals, for the integral Q_{125}.

$\mathbf{X_N}$	**Paths**	$\mathbf{c_{m,X}}$
F_2	$[\mu\rho\omega]$	$-6/(k_A k_B^2)$
G_3^B	$[\mu\rho\upsilon]$	$6/(k_A k_B)$
F_4	$[\mu\sigma]$, $[\nu\omega]$, $[\xi\rho\omega]$	$(6p - k_B^2)/(k_A k_B^2)$
G_5^B	$[\nu\upsilon]$, $[\xi\rho\upsilon]$	$-(k_B^2 + 6p)/(k_A k_B)$
F_6	$[\xi\sigma]$	$2p/k_A$

the resultant vertex, $\langle IJK\rangle$, is then given by the sum of weights, e.g., the above path would give $\langle i-3, j-3, k-4\rangle$. The valid paths for a particular integral are therefore the ones where $I = J = 0$, which translates to paths where the sum of orders of the first- and second-index edges are precisely i and j, respectively, with the first-index edges always traversed first. The order of an edge with respect to an index is the magnitude of its reduction in that index, e.g., μ-edges have order one in i, while σ-edges have order two in j. Only the ν-edges have a mixed order, which is one in both i and j. This almost completely determines the paths that need be considered, and is equivalent to generating all symbolic permutations within a class. This is an example of a combinatorial search, for which many efficient algorithms already exist.[32] There is an additional constraint, which somewhat simplifies the search: that υ and ω can only ever be the final edge, as these always end at a 'base' vertex, and ρ may never be the final edge, as then the accompanying σ term would have $j < 0$.

To give a concrete example, consider the starting vertex $\langle 125\rangle$. We need to reach the set of vertices $\langle 00N\rangle$ with N ranging from two to six. Only one possible path will give $N = 2$, as every edge must decrease the k-index, and this is $[\mu\rho\omega]$, corresponding to the constants $\mu_{125}\rho\omega$. Similarly, the only path to give $N = 6$ is $[\xi\sigma]$. All of the paths and the resultant coefficients are given in Table I. The more complex case of $\langle 226\rangle$ is shown schematically in the graph in Figure 2.Together, these demonstrate the reduction in complexity. The traversal of the graph and subsequent simplification of the algebraic terms can all be automated, resulting in integrals that involve a minimal number of summations of predefined quantities, allowing for optimised code to be generated.

B. Dealing with small exponents

The two main problems previously associated with recursive schemes for ECP integrals are a lack of efficiency, which has been dealt with above, and numerical issues concerning certain arguments of the Bessel functions. The latter problem is in fact inherent in all currently used methods, however; the method of Taylor expansion of the integral switches to using numerical quadrature when convergence of the expansion fails, while the half-numerical scheme defaults to a much larger grid and a different transformation of the integral limits when the desired accuracy is not achieved. In all cases, the problem is due to either very small or very large arguments of the Bessel functions, whereby the integrals themselves become small but non-vanishing. In particular, quadrature using the standard logarithmic transformation[33,34] struggles with large arguments, whence the width of the integrand becomes very small, while the Taylor series fails for very small arguments, where the integrand is at its most skewed. For the recurrence relations, it is also the latter instance that causes the most problems, as all terms involve some form of $1/k_A$ or $1/k_B$. Given that in any reasonable chemical system, A and B are likely to be roughly larger than one (Bohr), this translates to the case of very small exponents, where the definition of 'very small' is dependent on the arithmetic precision being employed.

The solution to this issue is to be found in the prescreening outlined earlier. Equation 24 is robust and accurate enough that, for sufficiently small values of the integral, it can give the correct result to within a reasonable desired precision. In the case of large k_A and k_B, it is simple to demonstrate that the integrand tends to a Gaussian, such that the prescreening becomes essentially exact. This is shown in the right-hand plot of Figure 1. For α or β tending to zero, the Bessel functions vanish unless they are $M_0(z)$, where they tend to unity. When coupled with the exponential decay, this means the value of the integral also becomes small, with the exception of the case where both Bessel functions are $M_0(z)$. However, this instance does not necessitate recursion, as the result can be written directly in terms of a single base integral. Given a tolerance of ϵ, if the prescreened value $\iota < \epsilon$ we skip the integral. If ι is accurate to within $\delta\%$, then we can take it to be the true value for $\iota < 100\epsilon/\delta$. For usual values of $\epsilon \sim 10^{-12}$, this should eliminate numerical problems for δ in the range 0.1 to 1. If stricter tolerance is required, the only options are to use high-precision arithmetic, for example by avoiding floating point representations, or to default to quadrature with a large

grid and a restricted integration interval.

As given, the prescreening value usually achieves precision within 1 to 35 percent. However, this can be greatly increased by either rescaling the value, or rescaling the exponent. The fitted Gaussian has two degrees of freedom - the center and the exponent - one of which is fixed by requiring that the value at the mode agrees exactly with that of the true distribution. We are then free to fit the exponent to any other point. As shown in Figure 1, the width of the distribution is overestimated most severely on the left hand side, which suggests fitting to a point $P - \Delta$, for some small $\Delta > 0$. The exponent to use in equation 25 can then be determined as

$$\gamma = -\frac{1}{\Delta^2} \ln \left(\frac{f(P - \Delta)}{f(P)} \right) \tag{42}$$

Note that as $f(z) \leq f(P)$ for all z, this will always give a positive exponent, as should be expected. In addition, taking the fitted point to the left of center will underestimate the width, unless very small Δ is used, while equivalently, taking the fitted point to the right of center will overestimate the width. This suggests one approach would be to take multiple such points on each side, and average the integrals in some way; this could then potentially be used to evaluate all integrals to within the desired precision.

Alternatively, we can observe the percentage deviation as a function of the exponent empirically, as shown in Figure 3 for β (symmetry of the integrand implies the same must apply for α). This seems to suggest the percentage deviation follows something approximating a Normal distribution, so that we can rescale the integral (once for each of α and β) as:

$$\tilde{\iota} = \frac{\iota}{1 + Y \exp(-o[(\log_{10} \alpha - O)^2 + (\log_{10} \beta - O)^2])} \tag{43}$$

where Y, o and O are the empirically determined amplitude, standard deviation, and mean of the error distribution above. A least-squares fitting designed to favour the most needed region (around 10^{-6} to 10^{-2}) gives these to be $Y = 34.5$, $o = 0.024$, and $O = -3.1$, the result of which is also shown in Figure 3.

V. RESULTS

In order to test the integration scheme, code was generated as described above capable of handling up to f-type basis functions, both in the orbital and ECP bases. This was then

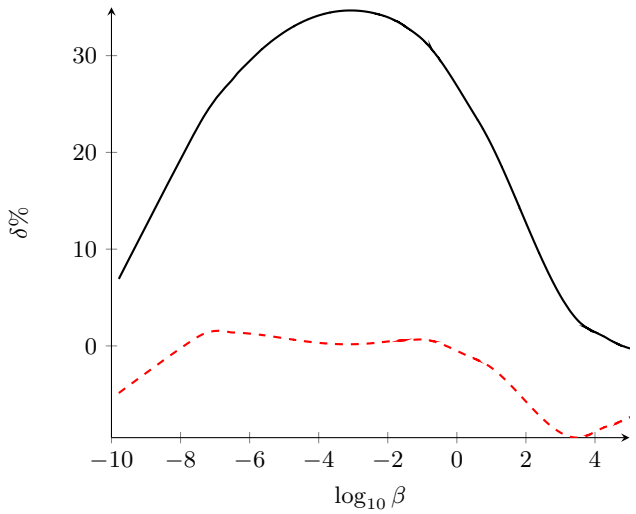

FIG. 3. The percentage deviation of the prescreening value of the integral from that calculated using the large quadrature grid, as a function of the exponent β. All other parameters were fixed to be 1.0. The solid black line is the value from equation 24, whilst the dashed red line is the rescaled value from equation 43. The results are from 10,000 randomly generated exponents, β, with the deviation taken as the average over all 50 Q_{ijk}.

manually checked and further optimised. For comparison, an adaptive Gauss-Chebyshev quadrature was implemented[35,36], utilising in the first instance a 256-point grid and the logarithmic transformation of Treutler and Ahlrichs[33,34], but defaulting to a 1024-point quadrature over primitives with a linear transformation when the former fails to converge. Both used a tolerance of 10^{-12}. This is as described in Ref. 25. The same prescreening routine was then applied to both of these, with the option of having no rescaling, integral rescaling with parameters as listed above, or exponent rescaling. In the latter case, a value of $\Delta = 0.34/\sqrt{p}$ was found to give the best results. Both approaches yield broadly similar precision, but in general the integral rescaling is more efficient as it does not require any further Bessel function evaluations. Therefore, this was chosen to be the default method in the recursive scheme. The code was implemented both as a standalone program, and as part of an in-house quantum chemistry code. For the benchmarking tests, a pseudo-random number generator was used to select parameters η, α, β, A, and B, before calculating Q_{ijk} for all relevant combinations of i, j, and k in the range zero to five. The exponents were chosen to be 10^n with n drawn from a Normal distribution with mean zero and standard deviation two, while A and B were drawn from uniform distributions on $[0.1, 10]$. The true

value of the integral was taken to be that from the aforementioned 1024-point quadrature, but with a tolerance of 10^{-14}.

For the tests on silver clusters, restricted Hartree-Fock (HF) and coupled cluster with singles and doubles excitations and perturbative triples, CCSD(T), calculations were performed with both cc-pVDZ-PP (VDZ-PP herein) and aug-cc-pVDZ-PP (aVDZ-PP) correlation consistent basis sets on the silver atoms[37], which use the ECP28MDF effective core potential[38]. Pure spherical harmonic functions were used throughout. Benchmark values were calculated using the MOLPRO 2015.1 suite of programs[39], to compare with the results from the in-house code. The lowest energy geometries for the Ag_n clusters were taken from the work of Duanmu and Truhlar[40], optimised using CCSD(T) for $n = 2$ to 4 and the N12 density functional for $n = 5, 6$[41]; the basis set used was aug-cc-pVQZ-PP[37]. All timings in this and the above were performed on a single processor.

A. Benchmarking and stability tests

The efficiency of the prescreening (without any rescaling) is demonstrated in Figure 4. This shows both how the prescreened value remains strictly greater than or equal to the true value, and the closeness of their agreement, as the plot is very near linear for the majority of values. Of the five million integrals, approximately 19% were below the chosen tolerance of 10^{-12}. While the bound appears to be less close in this regime, the important point is that the subsequent integrations are correctly avoided. Moreover, below the tolerance of the large quadrature (10^{-14}) the differences may be due to the limited precision. The validity of the prescreening did not significantly change upon changing the ijk indices of the integral, which is most likely due to the explicit determination of the value at the maximum. The starting guess for the mode was taken to be P_+ as defined earlier; using this, the iterations of equation 20 converged to within 0.01 in 2.24 cycles on average. In general, the fixed point equation converged in at most 3 iterations, regardless of the particular parameters or indices of the integral, demonstrating the robustness of the procedure. The cost can be further reduced by loosening the convergence criterion, with a choice of 0.1 performing similarly well and requiring only 1.9 cycles on average. However, this did very occasionally result in loss of the strictness of the bound.

To study the numerical stability of the new scheme, it suffices to look at how the absolute

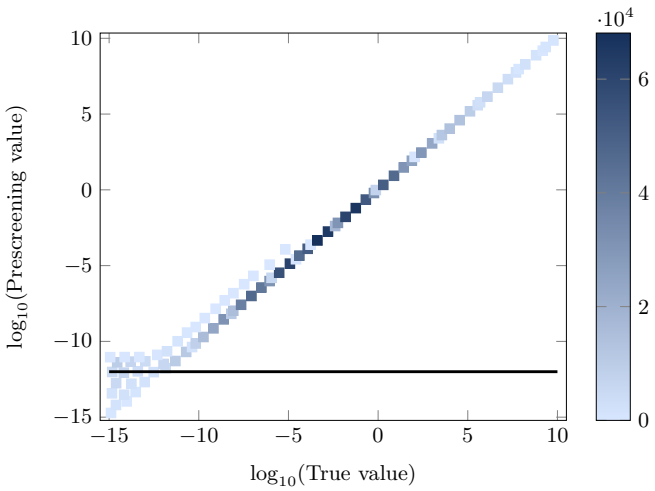

FIG. 4. A log-log plot of the integral value as determined by the prescreening procedure compared to that from the 1024-point quadrature, where the density indicates the number of integrals. Shown are the results from 100,000 randomly generated sets of parameters, evaluated for 50 different Q_{ijk}, ranging from Q_{002} to Q_{554}, restricted to even $i + j + k$. The black line indicates the desired prescreening threshold of 10^{-12}.

error in the integral (as compared to that from the large quadrature) varies with exponent. As has already been noted, the parameters A and B are constrained by the nature of the system, while symmetry means that considering α or β is equivalent. Therefore, we just allow β to vary, fixing all other parameters to unity. The results are shown in Figure 5. For the majority of exponents, all three schemes shown are well below the desired tolerance of 10^{-12}. We note that any differences between them below 10^{-14} again cannot be taken to be meaningful, as this was the cutoff for convergence of the reference value. The most notable feature is how the recursive- and quadrature-based integrations show reversed trends in stability. This agrees with the expectation outlined earlier: the latter struggles with large values of the exponent, where the distribution tends towards vanishing width, while the former has problems with very small exponents. Upon applying the scaled prescreening, however, it can be seen that the error is brought safely below the threshold. This is then the only method that gives stability across the entire range. It should be noted that in real basis sets the exponents are most likely to be found in the range $[10^{-5}, 10^{5}]$, such that the instabilities in the quadrature will be uncommon. For very large values of both α and β, though, failures in convergence are observed, which is why the procedure has the option

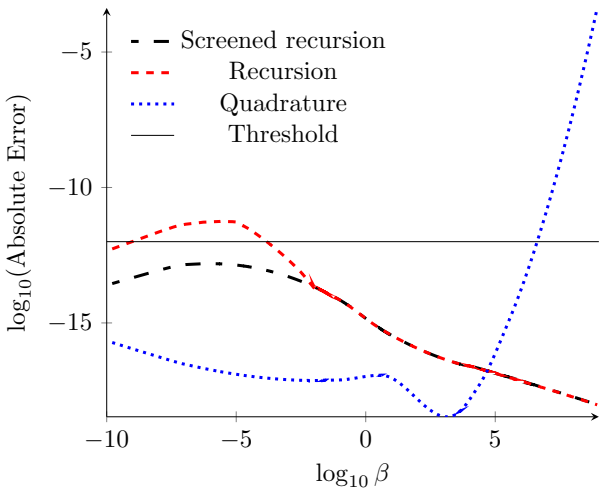

FIG. 5. A log-log plot of the absolute error in the integral (compared to that from the large-grid quadrature) for the recursive integration (with and without prescreening) and the 256-point quadrature. The values are from 10,000 randomly generated exponents, averaged over all 50 Q_{ijk}.

to switch to a larger quadrature over primitives. The figure shows errors averaged over all integrals for a given set of parameters, and thus does not show how stability depends on the integral indices. In general, the larger the value of $i + j + k$, the larger the error in all schemes, but particularly in the recursion, as is to be expected. However, the differences in error between Q_{002} and Q_{554} are roughly one order of magnitude (10^{-14} as compared to 10^{-13}), such that the overall deviation remains below 10^{-12} for the screened recursion scheme.

Finally, Figure 6 shows the speedups that can be achieved by using the prescreening, and by using the new integration scheme. When applied to the quadrature, prescreening results in modest savings of on average a factor of 1.5. The code-generated recursive method, however, offers savings of approximately two orders of magnitude. These timings are taken by cumulatively summing over the time taken for the five million integrals. In general, the higher the angular momenta, the less efficient the recursions are. However, the unrolling means that while Q_{554} takes on average three times as long as Q_{002}, it is still orders of magnitude faster than the quadrature.

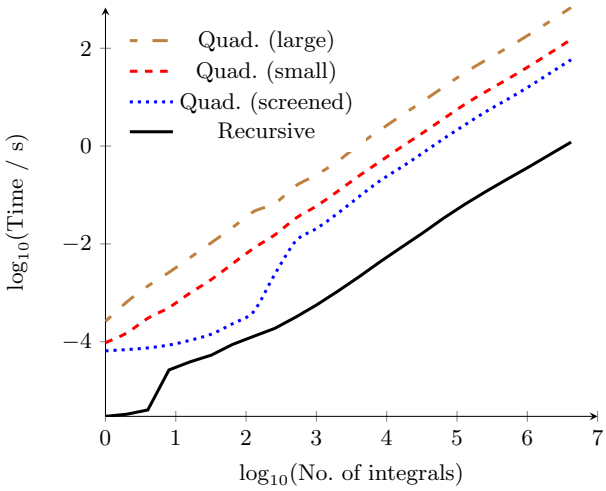

FIG. 6. The cumulative time taken to calculate a given number of integrals, for the large, small, and prescreened small quadratures, and the recursive scheme with scaled prescreening. As can be seen, the new methods are significantly more efficient. The accumulation is taken over the 100,000 randomly generated parameter sets, each used to calculate 50 Q_{ijk}, with ijk ranging from 002 to 554.

B. Tests on silver clusters

CCSD(T) single-point calculations on closed-shell silver clusters with up to six silver atoms were performed using both the VDZ-PP and aVDZ-PP basis sets. The results for the former, compared to calculations performed in MOLPRO, are shown in table II. As can be seen, in all instances the energy calculated using either integration scheme is identical to the MOLPRO value to within the threshold ($10^{-7}\mathrm{E}_h$) chosen for convergence of the energy. This demonstrates that neither the prescreening nor the recursion are resulting in any numerical issues overall. The results in the aVDZ-PP basis are very similar, and are given in the supplementary material. Moreover, it can be seen that there are significant time savings associated with the recursive scheme compared to the prescreened quadrature. The former is on average 32 (VDZ-PP) or 38 (aVDZ-PP) times faster than its counterpart. In fact, the speedups are such that the silver hexamer takes roughly the same amount of time in the new scheme as the dimer does using quadrature. This is despite the number of basis functions tripling.

This can be seen most clearly in Figure 7, where the scaling of the integration with the number of ECP centers is shown. We note that, as all atoms are the same, the number of

TABLE II. CCSD(T)/VDZ-PP energies for small, closed-shell silver clusters, with absolute errors, Δ/E_h,[a] for energies calculated using the screened recursion and quadrature schemes for the ECP integrals. In addition, total ECP integration times relative to Ag_2 in the recursive scheme (0.05 seconds) are shown.

Cluster	**Energy**	$\mathbf{\Delta}_{\text{recur.}}$	$\mathbf{\Delta}_{\text{quad.}}$	$\mathbf{t}_{\text{recur.}}$	$\mathbf{t}_{\text{quad.}}$
Ag_2	−292.72567	0	0	1.0	22.5
Ag_3^+	−438.89548	0	0	3.19	84.5
Ag_3^-	−439.15819	0	0	3.12	76.5
Ag_4	−585.49395	0	0	8.76	306.9
Ag_5^+	−731.68262	0	0	16.5	668.6
Ag_5^-	−731.94691	0	0	12.6	418.0
Ag_6	−878.29971	0	0	26.8	1080.2

[a] These were zero to within the convergence threshold of 10^{-7}.

centers also describes the number of basis functions - 38 and 54 per silver atom in VDZ-PP and aVDZ-PP respectively - and thus this is a well-defined measure of system size. As these are three-centre integrals, they formally scale cubically with system size. Power law fits suggest that this is broadly true, with powers of ~ 2.6 and 3.1 with and without prescreening, respectively. The difference in scaling between quadrature and recursion is negligible - applying prescreening improves both equally - but the prefactor for the latter is clearly significantly smaller.

VI. CONCLUSIONS

We have presented new, efficient schemes for both the prescreening and evaluation of the radial parts of integrals over ECPs. The prescreening yields speedups for both the most commonly used half-numerical integration routine, and for the newly proposed recursive routine, on the order of a factor of 1.5 in both cases. This is largely due to the closeness of the bound. Moreover, it has been shown that it is possible to use this not simply as a prescreening method, but as a way to evaluate the integrals. Initial attempts at doing so result in a numerically stable and highly efficient recursive integration scheme, almost

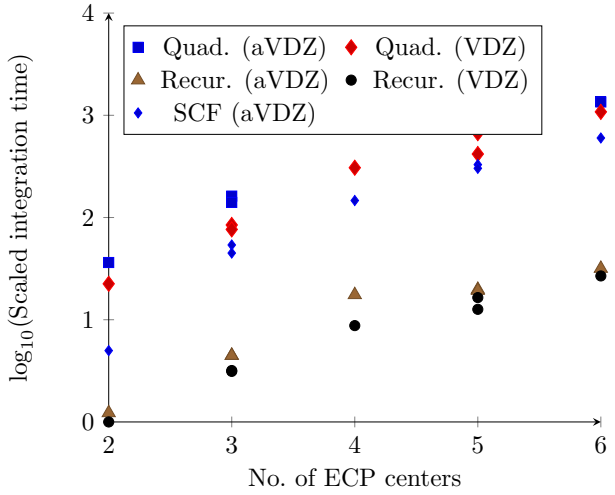

FIG. 7. Shown are scaled timings (relative to Ag_2 in the VDZ-PP basis using the recursive scheme, 0.05 seconds) for the ECP integration steps in calculations on closed-shell silver clusters. The number of ECP centres also corresponds to the number of basis functions (38 and 54 per silver atom for VDZ-PP and aVDZ-PP, respectively). Results are given for the screened quadrature with VDZ-PP (red diamonds) and aVDZ-PP (blue squares), and similarly for the recursive scheme with scaled prescreening (black circles for VDZ-PP, gray triangles for aVDZ-PP). In addition, the timings for a single, integral-direct SCF iteration in the aVDZ-PP basis are shown for comparison.

two orders of magnitude faster than the quadrature-based method. The careful unrolling of the recursion relations and optimised code generation, coupled with an effective method of prescreening, have allowed for this, most notably eliminating the numerical instabilities of previous recursive methods. Tests on silver clusters have demonstrated that the scheme gives the same accuracy at much reduced cost as current methods, while the prescreening reduces the scaling with respect to system size. The approach is independent of the angular momenta involved, and thus spin-orbit coupling integrals and analytic derivatives can be treated identically.

SUPPLEMENTARY MATERIAL

See supplementary material for proof of the unimodality of the integrand, derivation of base integrals, special cases of the integrals and results for CCSD(T)/aVDZ-PP calculations on silver clusters.

ACKNOWLEDGMENTS

The authors thank the Engineering and Physical Sciences Research Council (UK) for a postgraduate studentship awarded to R.A.S. and project funding (EP/N02253X/1).

REFERENCES

[1]A. Tajti, P. G. Szalay, A. G. Császár, M. Kállay, J. Gauss, E. F. Valeev, B. A. Flowers, J. Vázquez, and J. F. Stanton, J. Chem. Phys. **121**, 11599 (2004).

[2]A. Karton, E. Rabinovich, J. M. L. Martin, and B. Ruscic, J. Chem. Phys. **125**, 144108 (2006).

[3]W. Klopper, F. R. Manby, S. Ten-No, and E. F. Valeev, Int. Rev. Phys. Chem. **25**, 427 (2006).

[4]H.-J. Werner, F. R. Manby, and P. J. Knowles, J. Chem. Phys. **118**, 8149 (2003).

[5]S. Saebo and P. Pulay, Annu. Rev. Phys. Chem. **44**, 213 (1993).

[6]H. Hellmann, J. Chem. Phys. **3**, 61 (1935).

[7]H. Hellmann and W. Kassatotschkin, J. Chem. Phys. **4**, 324 (1936).

[8]P. Gombás, Z. Phys. **94**, 473 (1935).

[9]J. C. Phillips and L. Kleinman, Phys. Rev. **116**, 287 (1959).

[10]P. Pyykkö, Chem. Rev. **88**, 563 (1988).

[11]J. D. Weeks and S. A. Rice, J. Chem. Phys. **49**, 2741 (1968).

[12]M. Dolg, in *Modern methods and algorithms of quantum chemistry*, edited by J. Grotendorst (John von Neumann Institute for Computing, Jülich, 2000) pp. 507–540.

[13]P. Pyykkö, Adv. Quantum Chem. **11**, 353 (1978).

[14]K. S. Pitzer, Acc. Chem. Res. **12**, 271 (1979).

[15]S.-g. Wang, W. Liu, and W. H. E. Schwarz, J. Phys. Chem. A **106**, 795 (2002).

[16]P. Pyykkö, Chem. Rev. **112**, 371 (2012).

[17]P. Schwerdtfeger, L. F. Pašteka, A. Punnett, and P. O. Bowman, Nucl. Phys. A **944**, 551 (2015).

[18]W. M. Huo and Y.-K. Kim, Chem. Phys. Lett. **319**, 576 (2000).

[19]S. O. Odoh and G. Schreckenbach, J. Phys. Chem. A **114**, 1957 (2010).

[20]W. A. Goddard, Phys. Rev. **174**, 659 (1968).

[21]L. R. Kahn and W. A. Goddard, J. Chem. Phys. **56**, 2685 (1972).

[22]L. R. Kahn, P. Baybutt, and D. G. Truhlar, J. Chem. Phys. **65**, 3826 (1976).

[23]L. E. McMurchie and E. R. Davidson, J. Comput. Phys. **44**, 289 (1981).

[24]C.-K. Skylaris, L. Gagliardi, N. C. Handy, A. G. Ioannou, S. Spencer, A. Willetts, and A. M. Simper, Chemical Physics Letters **296**, 445 (1998).

[25]R. Flores-Moreno, R. J. Alvarez-Mendez, A. Vela, and A. M. Köster, J. Comput. Chem. **27**, 1009 (2006).

[26]C. Song, L.-P. Wang, T. Sachse, J. Preiß, M. Presselt, and T. J. Martínez, J. Chem. Phys. **143**, 014114 (2015).

[27]C. Song, L.-P. Wang, and T. J. Martínez, J. Chem. Theory Comput. **12**, 92 (2016).

[28]M. Kolář, Comput. Phys. Commun. **23**, 275 (1981).

[29]B. M. Bode and M. S. Gordon, J. Chem. Phys. **111**, 8778 (1999).

[30]M. Abramowitz, *Handbook of Mathematical Functions, With Formulas, Graphs, and Mathematical Tables,* (Dover Publications, Incorporated, New York, 1974).

[31]G. B. Arfken, H. J. Weber, and F. E. Harris, *Mathematical Methods for Physicists: A Comprehensive Guide* (Academic Press, Cambridge, Massachusetts, 2012).

[32]Y. Hamadi, *Combinatorial Search: From Algorithms to Systems* (Springer, Berlin, Heidelberg, 2013).

[33]O. Treutler and R. Ahlrichs, J. Chem. Phys. **102**, 346 (1995).

[34]M. Krack and A. M. Köster, J. Chem. Phys. **108**, 3226 (1998).

[35]J. Pérez-Jordá, E. San-Fabián, and F. Moscardó, Comput. Phys. Commun. **70**, 271 (1992).

[36]J. Pérez-Jordá and E. San-Fabián, Comput. Phys. Commun. **77**, 46 (1993).

[37]K. A. Peterson and C. Puzzarini, Theor. Chem. Acc. **114**, 283 (2005).

[38]D. Figgen, G. Rauhut, M. Dolg, and H. Stoll, Chem. Phys. **311**, 227 (2005).

[39]H.-J. Werner, P. J. Knowles, G. Knizia, F. R. Manby, M. Schütz, P. Celani, W. Györffy, D. Kats, T. Korona, R. Lindh, A. Mitrushenkov, G. Rauhut, K. R. Shamasundar, T. B. Adler, R. D. Amos, A. Bernhardsson, A. Berning, D. L. Cooper, M. J. O. Deegan, A. J. Dobbyn, F. Eckert, E. Goll, C. Hampel, A. Hesselmann, G. Hetzer, T. Hrenar, G. Jansen, C. Köppl, Y. Liu, A. W. Lloyd, R. A. Mata, A. J. May, S. J. McNicholas, W. Meyer, M. E. Mura, A. Nicklass, D. P. O'Neill, P. Palmieri, D. Peng, K. Pflüger, R. Pitzer, M. Reiher, T. Shiozaki, H. Stoll, A. J. Stone, R. Tarroni, T. Thorsteinsson, and M. Wang, "MOLPRO, version 2015.1, a package of ab initio programs," (2015), see http://www.molpro.net.

[40]K. Duanmu and D. G. Truhlar, J. Phys. Chem. C **119**, 9617 (2015).

[41]R. Peverati and D. G. Truhlar, J. Chem. Theory Comput. **8**, 2310 (2012).